



Mononuclear, homo- and hetero-binuclear complexes of 1-(5-(1-(2-aminophenylimino)ethyl)-2,4-dihydroxyphenyl)ethanone: synthesis, magnetic, spectral, antimicrobial, antioxidant, and antitumor studies

Magdy Shebl

To cite this article: Magdy Shebl (2016) Mononuclear, homo- and hetero-binuclear complexes of 1-(5-(1-(2-aminophenylimino)ethyl)-2,4-dihydroxyphenyl)ethanone: synthesis, magnetic, spectral, antimicrobial, antioxidant, and antitumor studies, Journal of Coordination Chemistry, 69:2, 199-214, DOI: [10.1080/00958972.2015.1116688](https://doi.org/10.1080/00958972.2015.1116688)

To link to this article: <http://dx.doi.org/10.1080/00958972.2015.1116688>

 View supplementary material [↗](#)

 Accepted author version posted online: 10 Nov 2015.
Published online: 22 Jan 2016.

 Submit your article to this journal [↗](#)

 Article views: 6

 View related articles [↗](#)

 View Crossmark data [↗](#)

Mononuclear, homo- and hetero-binuclear complexes of 1-(5-(1-(2-aminophenylimino)ethyl)-2,4-dihydroxyphenyl) ethanone: synthesis, magnetic, spectral, antimicrobial, antioxidant, and antitumor studies

Magdy Shebl

Faculty of Education, Department of Chemistry, Ain Shams University, Cairo, Egypt

ABSTRACT

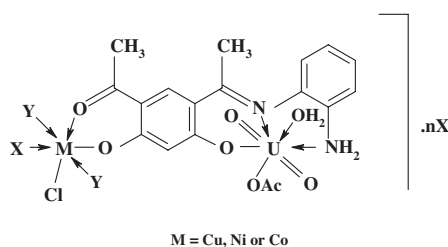
A new Schiff base, H_2L , was prepared by condensation of 4,6-diacetylresorcinol with *o*-phenylenediamine in molar ratio 1 : 1. The ligand reacted with copper(II), nickel(II), cobalt(II), iron(III), zinc(II), oxovanadium(IV), and dioxouranium(VI) ions in the absence and presence of LiOH to yield mononuclear and homobinuclear complexes. The mononuclear dioxouranium(VI) complex $[(HL)(UO_2)(OAc)(H_2O)] \cdot 5H_2O$ was used to synthesize heterobinuclear complexes. The ligand and its metal complexes were characterized by elemental analyses, IR, 1H -, and ^{13}C -NMR, electronic, ESR and mass spectra, conductivity, and magnetic susceptibility measurements as well as thermal analysis. In the absence of LiOH, mononuclear complexes (**1**, **4**, and **9**) were obtained; in the presence of LiOH, binuclear complexes (**3**, **5**, **7**, and **10**) as well as mononuclear complexes (**2**, **6**, and **8**) were obtained. In the mononuclear complexes, the coordinating sites are the phenolic oxygen, azomethine nitrogen, and amino nitrogen. In addition to these coordinating sites, the free carbonyl and phenolic OH are involved in coordination in binuclear complexes. The metal complexes exhibited octahedral, tetrahedral, and square planar geometries while the uranium is seven-coordinate. The antimicrobial and antioxidant activities of the ligand and its complexes were investigated. The ligand and the metal complexes showed antitumor activity against Ehrlich Acites Carcinoma.

ARTICLE HISTORY

Received 29 January 2015
Accepted 15 October 2015

KEYWORDS

Schiff base ligand; mono- and binuclear complexes; 4,6-diacetylresorcinol; ^{13}C -NMR spectra; ESR spectra; antimicrobial; antioxidant and antitumor activities



1. Introduction

Coordination chemistry of Schiff base ligands has been the subject of interest with various applications as antibacterial, antifungal, antioxidant and antitumor agents [1–3], and oxygen carriers [4, 5]. Due to their important role in catalysis and magnetism [6–9], many complexes have been given attention [10].

Binuclear complexes particularly heterobinuclear systems [11, 12] are of special interest due to their relevance to molecular magnetism, material sciences, industrial catalysis, and bioinorganic chemistry [13], and they are ubiquitous in nature as active sites in a variety of metalloenzymes [14–17].

4,6-Diacetylresorcinol (DAR) is a starting material for construction of polydentate ligands [18–24]. In our previous studies, metal complexes of different polydentate ligands derived from 4,6-diacetylresorcinol [25–29] were synthesized and characterized. These ligands were used to synthesize homopolynuclear complexes with different modes of bonding. However, no heterobinuclear complexes have been synthesized or studied biologically.

The present work is an extension to our work and is devoted to the synthesis of the new Schiff base ligand 1-(5-(1-(2-aminophenylimino)ethyl)-2,4-dihydroxyphenyl)ethanone by condensation of 4,6-diacetylresorcinol with *o*-phenylenediamine in the molar ratio 1:1. Reactions of the Schiff base with copper(II), nickel(II), cobalt(II), iron(III), zinc(II), oxovanadium(IV), and dioxouranium(VI) ions in the absence and presence of LiOH were studied. The dioxouranium(VI) complex (**9**) was used as a ligand towards copper(II), nickel(II), cobalt(II), and iron(III) ions, yielding heterobinuclear complexes. The ligand and its metal complexes were characterized by elemental analyses, IR, ¹H-, and ¹³C-NMR, electronic, ESR and mass spectra, conductivity, and magnetic susceptibility measurements as well as thermal analysis. The biological activity of the ligand and its complexes was screened against selected bacteria and fungi. The antioxidant and antitumor activities of the ligand and its metal complexes were investigated.

2. Experimental

2.1. Reagents and materials

4,6-Diacetylresorcinol was prepared as cited in the literature [19]. Copper(II), nickel(II), cobalt(II), and iron(III) were used as nitrate salts and obtained from Merck or BDH. Zinc(II) and dioxouranium(VI) ions were used as acetate salts, while the oxovanadium(IV) was used as the sulfate and were from Merck or Analar. *o*-Phenylenediamine, lithium hydroxide, nitric acid, ammonium hydroxide, metal indicators, and EDTA disodium salt were from BDH or Merck. Organic solvents (ethanol, absolute ethanol, methanol, diethylether, dimethylformamide (DMF), and dimethylsulfoxide (DMSO)) were reagent grade chemicals and were used without purification.

2.2. Synthesis of the Schiff base H₂L

The Schiff base H₂L was synthesized by adding 4,6-diacetylresorcinol (1.94 g, 10.0 mmol) dissolved in hot absolute ethanol (30 mL) to *o*-phenylenediamine (1.08 g, 10.0 mmol) in absolute ethanol (30 mL). The reaction mixture was heated to reflux for 6 h. The obtained yellow product was filtered and washed with ethanol then diethylether, air dried and recrystallized from ethanol. The crystalline ligand was kept in a desiccator until used. The yield was 2.14 g (75%). The melting point for H₂L was 206 °C. The reaction for the formation of H₂L is illustrated in Scheme 1.

2.3. Synthesis of the metal complexes

An ethanolic solution of the metal salt (30 mL) was added gradually to ethanolic solution of H₂L (40 mL) in molar ratio 1:1 (without using LiOH) and 2:1; M:L (in the presence of LiOH). The dioxouranium(VI) complexes were prepared in methanol as uranyl acetate is more soluble in this solvent; water was added to ensure complete dissolution of the metal salt in case of oxovanadium(IV) complex. Nickel(II), iron(III), zinc(II), and oxovanadium(IV) complexes were prepared successfully only in the presence of

LiOH. The reaction mixture was heated to reflux for 8 h. The resulting precipitates were filtered, washed with ethanol or methanol then diethylether, and finally air dried. The following detailed preparations are given as examples and the other complexes were obtained similarly.

2.3.1. Synthesis of [(HL)Cu(EtOH)](NO₃) (1)

About 0.328 g (1.41 mmol) of Cu(NO₃)₂·2.5H₂O dissolved in 30 mL ethanol was added gradually with constant stirring to the solution of H₂L (0.4 g, 1.41 mmol) in ethanol (30 mL). The reaction mixture was heated to reflux for 8 h giving a brown precipitate which was filtered, washed several times with small amounts of ethanol then diethylether and finally air dried. The yield was 0.258 g (40%), m.p. >300 °C.

2.3.2. Synthesis of [(HL)Cu(NO₃)(H₂O)₂]-EtOH (2)

About 0.118 g (2.81 mmol) of LiOH·H₂O dissolved in minimum distilled water (5 mL) was added gradually with constant stirring to solution of H₂L (0.4 g, 1.41 mmol) in ethanol (30 mL), then 0.656 g (2.82 mmol) of Cu(NO₃)₂·2.5H₂O dissolved in 30 mL ethanol was added to the mixture. The reaction mixture was heated to reflux for 8 h giving a dark brown precipitate which was filtered, washed several times with small amounts of distilled water, ethanol then diethylether, and finally air dried. The yield was 0.52 g (75%), m.p. 230 °C.

2.3.3. Synthesis of [(L)(UO₂)Cu(OAc)Cl(H₂O)(MeOH)]·MeOH (11)

About 0.07 g (1.67 mmol) of LiOH·H₂O dissolved in minimum distilled water (5 mL) was added gradually with constant stirring to **9** (1.2 g, 1.67 mmol), suspended in methanol (40 mL) and 0.225 g (1.67 mmol) of CuCl₂ dissolved in 30 mL methanol was added to the mixture. The reaction mixture was heated to reflux for 12 h giving a dark olive green precipitate which was filtered, washed several times with small amounts of distilled water, methanol then diethylether, and finally air dried. The yield was 0.75 g (57%), m.p. >300 °C.

2.4. Analytical and physical measurements

Elemental analyses were carried out using a Vario El-Elementar at the Ministry of Defense, Chemical War Department. Melting points of the ligand and its metal complexes were determined using a Stuart melting point instrument. Analyses of the metals followed dissolution of the solid complex in concentrated HNO₃, neutralizing the diluted aqueous solutions with ammonia (except iron(III) complex) and titrating the metal solutions with EDTA. IR spectra were recorded using KBr disks on a FT IR Nicolet IS10 spectrometer. Electronic spectra were recorded as solutions in DMF or Nujol mulls on a Jasco UV-vis spectrophotometer model V-550 UV-Vis. ¹H- and ¹³C-NMR spectra were recorded at room temperature using a Bruker WP 200 SY spectrometer. Deuterated dimethylsulfoxide (DMSO-d₆) was used as a solvent and tetramethylsilane (TMS) as an internal reference. The chemical shifts (δ) are given downfield relative to TMS. D₂O was added to test for deuteration of the samples. ESR spectra were recorded at an Elexsys, E500, Bruker company. The magnetic field was calibrated with 2,2'-diphenyl-1-picrylhydrazyl (DPPH) purchased from Aldrich. Mass spectra were recorded at 70 eV on a Gas chromatographic GCMSqp 1000 ex Shimadzu instrument. The magnetic susceptibility measurements were carried out at room temperature using a magnetic susceptibility balance, Johnson Matthey, Alfa product, Model No (MKI). Effective magnetic moments were calculated from the expression $\mu_{\text{eff}} = 2.828 (\chi_{\text{M}} \cdot T)^{1/2}$ (BM), where χ_{M} is the molar susceptibility corrected using Pascal's constants for the diamagnetism of all atoms in the compounds [30]. Molar conductivities of 10⁻³ M solutions of the solid complexes in DMF were measured on a Corning conductivity meter NY 14831 model 441. TGA-measurements were carried out from room temperature to 800 °C at a heating rate of 10 °C min⁻¹ on a Shimadzu-50 thermal analyzer.

2.5. Antimicrobial activity

The standardized disk-agar diffusion method [31, 32] was followed to determine the activity of the synthesized compounds against *Staphylococcus aureus* (ATCC 25923) and *Bacillus subtilis* (ATCC 6635) as Gram-positive bacteria, *Salmonella typhimurium* (ATCC 14028) and *Escherichia coli* (ATCC 25922) as Gram-negative bacteria and *Candida albicans* (ATCC 10231) and *Aspergillus fumigatus* as fungi. The antibiotic chloramphenicol was used as reference in the case of Gram-positive bacteria, cephalothin in the case of Gram-negative bacteria, and cycloheximide in the case of fungi.

2.5.1. Preparation of the tested compound

The tested compounds were dissolved in DMF and prepared in two concentrations; 100 and 50 mg mL⁻¹ and then 10 µL of each preparation was dropped on a 6 mm disk and the concentrations became 1 and 0.5 mg disk⁻¹, respectively. In the case of insoluble compounds, the compounds were suspended in DMF and vortexed then processed.

2.5.2. Testing for antibacterial and yeasts activity

Bacterial cultures were grown in nutrient broth medium at 30 °C. After 16 h of growth, each micro-organism, at a concentration of 10⁸ cells mL⁻¹, was inoculated on the surface of Mueller-Hinton agar plates using a sterile cotton swab. Subsequently, uniform size filter paper disks (6-mm in diameter) were impregnated by equal volume (10 µL) from the specific concentration of dissolved compounds and carefully placed on the surface of each inoculated plate. The plates were incubated in the upright position at 36 °C for 24 h. Three replicates were carried out for each extract against each test organism. Simultaneously, addition of the respective solvent instead of dissolved compound was carried out as negative controls. After incubation, the diameters of the growth inhibition zones formed around the disk were measured with transparent ruler in millimeter, averaged and the mean values were tabulated.

2.5.3. Testing for antifungal activity

Active inoculum for experiments was prepared by transferring many loopfuls of spores from the stock cultures to test tubes of sterile distilled water that were agitated and diluted with sterile distilled water to achieve optical density corresponding to 2.0×10^5 spore mL⁻¹. Inoculum of 0.1% suspension was swabbed uniformly and the inoculum was allowed to dry for 5 min; then the same procedure was followed as described above.

2.5.4. Determination of minimum inhibitory concentration (MIC)

MIC is the lowest concentration of an antimicrobial compound that will inhibit the visible growth of a micro-organism after overnight incubation. MIC values of the synthesized compounds were determined using agar dilution technique [33]. Each compound with an antimicrobial effect shown in the disk diffusion test was further diluted with DMF to 25.6, 12.8, 6.4, 3.2, 1.6, 0.8, 0.4, 0.2, and 0.1 mg mL⁻¹, respectively. The concentrations of the compounds became 256, 128, 64, 32, 16, 8, 4, 2, and 1 µg mL⁻¹, respectively. Then 100 µL of each diluted compound was mixed with 10 ml of cooled (50 °C) melted Mueller-Hinton agar and 10 µL of specific microbial culture (at concentration of 10⁸ cells mL⁻¹), which were grown in nutrient broth medium for 16 h at 30 °C then plated into a 6-cm sterile Petri dish. Each dilution was prepared in duplicate. Each concentration was prepared for two dishes. All plates were incubated at 33 °C for 24 h. MIC of each compound was measured from the plate with the lowest concentration with no visible growth of specific organism.

2.6. Antioxidant activity

The method used by Takao *et al.* [34] was adopted with suitable modifications. DPPH (8 mg) was dissolved in methanol (100 mL) to obtain a concentration of 80 µg mL⁻¹. Serial dilutions were carried out with the stock solutions (4 mM) of the compounds in methanol to obtain concentrations of

2×10^{-4} – 0.25×10^{-4} M. Diluted solutions (2 mL each) were mixed with DPPH (2 mL) and allowed to stand for 30 and 60 min for any reaction to occur. The absorbance was recorded at 517 nm. The experiment was performed in triplicate and the average absorbance was noted for each concentration. The IC_{50} value, which is the concentration of the test compound that reduces 50% of the initial free radical concentration, was calculated as μM . Ascorbic acid was used as reference standard. Control sample was prepared containing the same volume without test compounds and reference compounds. The radical-scavenging activity of the tested samples, expressed as percentage inhibition of DPPH, was calculated according to the formula $IC(\%) = [(A_0 - A_t)/A_0] \times 100$, where A_t is the absorbance value of the tested sample and A_0 is the absorbance value of blank sample, at a particular time. Percent inhibitions after 30 and 60 min were plotted against concentration, and the equation for the line was used to obtain the IC_{50} value. A lower IC_{50} value indicates greater antioxidant activity.

2.7. Cytotoxicity assay

The antitumor activity of the Schiff base and its complexes was tested on Ehrlich Ascites Carcinoma (E.A.C.) according to the literature method [35]. A set of sterile test tubes was used, where 2.5×10^5 tumor cells per mL were suspended in phosphate buffer saline. Three tubes with three different concentrations for each compound (25, 50, and $100 \mu\text{g mL}^{-1}$ DMSO) were made and 2.5×10^5 tumor cells were added for each tube. The tubes were kept for 2 h at 37°C . The samples were taken volume by volume with trypan blue on slides and were covered and examined under the microscope. Dead cells were stained blue and live cells were not stained. Then the percentage of non-viable cells was calculated.

3. Results and discussion

3.1. The Schiff base H_2L

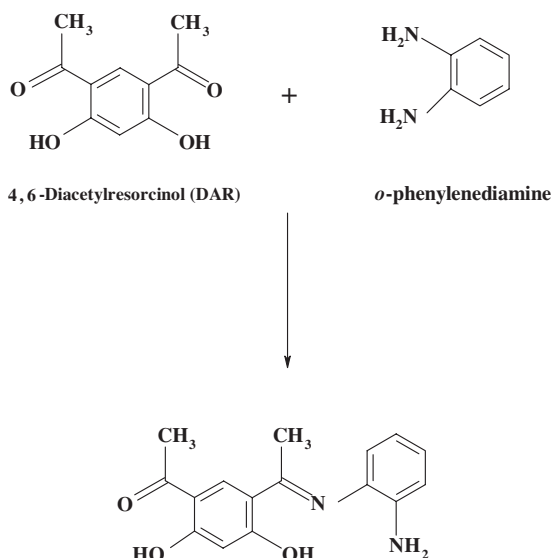
The Schiff base H_2L was prepared by condensation of 4,6-diacetylresorcinol with *o*-phenylenediamine in the molar ratio 1 : 1. The analytical and physical data of H_2L and its metal complexes are listed in Table S1. The results of the elemental analyses are in agreement with the proposed formulas.

The characteristic infrared spectral data of H_2L and its metal complexes are listed in Table S2. The IR spectrum of H_2L showed a broad band at 3426 cm^{-1} assigned to $\nu(\text{OH})$ and two bands at 3372 and 3215 cm^{-1} assigned to ν_{as} and ν_{s} of the amino group, respectively; strong bands at 1629 and 1595 cm^{-1} may be attributed to $\nu(\text{C}=\text{O})$ and $\nu(\text{C}=\text{N})$, respectively.

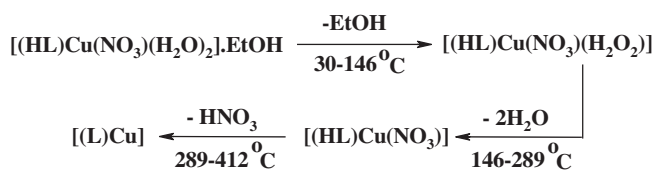
Electronic spectral data of H_2L (Table S3) were recorded in DMF solution. Four absorption bands at 268 nm, 312 nm, 350 nm, and 402 nm were observed. The first two bands correspond to ${}^1L_a \rightarrow {}^1A_1$ and ${}^1L_b \rightarrow {}^1A_1$ transitions of the phenyl ring [36]. The third band corresponds to the $\pi \rightarrow \pi^*$ transition of the azomethine and carbonyl groups while the last band corresponds to the $n \rightarrow \pi^*$ transition which is overlapped with the intermolecular charge-transfer (CT) from the phenyl ring [37, 38].

${}^1\text{H-NMR}$ spectral data (δ ppm) of the ligand relative to TMS (0 ppm) in $\text{DMSO-}d_6$ are listed in Table S4. The signals observed at 16.94 and 12.72 ppm may be assigned to the hydrogen-bonded phenolic $-\text{OH}$ [1, 26, 27, 29] with two different environments around the phenolic $-\text{OH}$ [39]. Signals at 4.92 ppm and in the range of 2.4–2.65 ppm may be assigned to the $-\text{NH}_2$ and CH_3 protons, respectively. Finally, the signals due to aromatic protons are 6.26–8.42 ppm. Assignment of the ${}^{13}\text{C-NMR}$ spectral data of H_2L (Figure S1) is based on ${}^{13}\text{C}$ shifts in similar Schiff bases [23]. The signals at 203.2 ppm, 174.1 ppm, 166 ppm, and 141.2 ppm may be assigned to $(\text{C}=\text{O})$, $(\text{C}=\text{N})$ and the two $(\text{C}-\text{OH})$ phenolic carbons, respectively. The methyl groups were between 27.9 and 17 ppm. Finally, aromatic carbons were observed between 103.9 and 137.9 ppm.

The mass spectrum of H_2L (Figure S2) showed the molecular ion peak at m/e 284, confirming its formula weight (F.W. 284.32). The mass fragmentation pattern shown in Scheme S1 supported the suggested structure of the ligand.



Scheme 1. Synthesis of H₂L.



Scheme 2. Thermal degradation pattern of [(HL)Cu(NO₃)(H₂O)₂]·EtOH (**2**) from 30 to 412 °C.

3.2. Characterization of the metal complexes

H₂L was allowed to react with copper(II), nickel(II), cobalt(II), iron(III), zinc(II), oxovanadium(IV), and dioxouranium(VI) ions. These reactions were repeated in the presence of LiOH to affect deprotonation of the ligand. The prepared complexes are stable at room temperature, non-hygroscopic, and insoluble in water and most common organic solvents. The analytical and physical data of the metal complexes are listed in Table S1.

3.2.1. IR spectra

IR spectral data of the metal complexes (Table S2) exhibit changes in the frequencies of the functional groups when compared to the spectrum of the ligand. These can be correlated to the specific coordination positions of the ligand. Some additional bands that appear in the spectra of the metal complexes can be correlated to metal coordinated positions.

There are four features in the IR spectra of the complexes. The first is the shift of the stretching frequencies of the azomethine $\nu(\text{C}=\text{N})$ group of the metal complexes to lower frequencies compared with the free ligand band at 1595 cm⁻¹, which may be due to coordination of the azomethine group to metal ions. Similarly, bands assigned to $\nu(\text{NH}_2)$ were shifted to lower frequencies in the complexes, indicating involvement of the amino group in chelation [40]. The $\nu(\text{C}=\text{O})$ of the free ligand at 1629 cm⁻¹ shifted to lower frequencies in the binuclear complexes, suggesting participation of the carbonyl group in chelation [41–43]. However, in the mononuclear complexes, no lowering of the $\nu(\text{C}=\text{O})$ band was observed, suggesting that metal carbonyl oxygen linkage is absent [29]. The second feature is the broad bands at

3335–3446 cm^{-1} which can be assigned to the stretching frequencies of $\nu(\text{OH})$ of alcohol, OH-phenolic, and/or water molecules associated to the complexes which are also confirmed by elemental and thermal analyses. The third feature is about nitrate and acetate anions as they are either coordinated or uncoordinated in their complexes. Complexes **1** and **4** showed new bands at 1369–1384 and 903–904 cm^{-1} which can be assigned to ionic NO_3^- [18], indicating the ionic nature of these complexes. Complex **2** showed new bands at 1299 and 1055 cm^{-1} which can be assigned to monodentate NO_3^- [44]. These IR spectral data were supported by conductance data. For **7**, **9**, and **11–14**, new bands characteristic for $\nu_{\text{asym}}(\text{COO}^-)$ and $\nu_{\text{sym}}(\text{COO}^-)$ of acetate were observed at 1638–1669 and 1392–1415 cm^{-1} , respectively [1, 45, 46]. The higher difference (223–267 cm^{-1}) between the two bands indicates monodentate acetate [1, 45, 46]. The fourth feature includes bands related to metal ions where the characteristic $\nu(\text{V}=\text{O})$ is observed in the IR spectrum of the oxovanadium(IV) complex (**8**) at 952 cm^{-1} [47, 48]. Also, the dioxouranium(VI) complexes (**9–14**) showed strong absorptions at 903–914 cm^{-1} which can be assigned to the antisymmetric $\nu_3(\text{O}=\text{U}=\text{O})$ vibration [26, 49, 50]. The values of $\nu(\text{V}=\text{O})$ and $\nu(\text{O}=\text{U}=\text{O})$ are used to calculate the force constant (F) of ($\text{V}=\text{O}$) and ($\text{O}=\text{U}=\text{O}$) by the method of McGlynn and Smith [51]: $(\nu)^2 = (1307)^2(F_{\text{M-O}})/14.103$. The calculated force constant for the oxovanadium(IV) and dioxouranium(VI) complexes are 7.482 and 6.732–6.897 $\text{mdyn } \text{\AA}^{-1}$, respectively. The M–O distance is also calculated by substitution in Jones relation [52]: $R_{\text{M-O}} = 1.08(F_{\text{M-O}})^{-1/3} + 1.17$. The values of $R_{\text{M-O}}$ for oxovanadium(IV) and dioxouranium(VI) complexes are 1.722 and 1.737–1.742 \AA , respectively. The calculated $F_{\text{M-O}}$ and $R_{\text{M-O}}$ values fall in the usual range for the oxovanadium(IV) and dioxouranium(VI) complexes [1, 47]. New bands at 592–615 and 412–486 cm^{-1} may be assigned to stretching frequencies of $\nu(\text{M}-\text{O})$ and $\nu(\text{M}-\text{N})$, respectively [25, 27, 29, 47, 53].

3.2.2. Conductivity measurements

The molar conductivities of the complexes (Table S3) showed that all complexes have non-electrolytic nature except **1** and **4** which gave molar conductance values of 90 and 77 $\Omega^{-1} \text{cm}^2 \text{mol}^{-1}$, respectively, suggesting their 1 : 1 electrolytic nature [54]. This is consistent with the infrared data that showed the presence of an ionic nitrate.

3.2.3. Magnetic measurements, electronic, and ESR spectra

The magnetic properties of the complexes, in addition to electronic spectral data, provide valuable information for distinguishing their stereochemistry. The electronic spectral measurements of all metal complexes (Table S3) were carried out as DMF solutions and Nujol mulls. The spectra and position of the bands of all complexes in DMF solutions are approximately the same as those recorded as Nujol mulls, reflecting insignificant effect of DMF on the complex configuration. This also proves that the same species is present both in the solid and the solution states, indicating that the complexes retain their integrity in solutions [55, 56]. Comparison of the spectrum of the free ligand with its complexes showed that bands of the free ligand were slightly shifted to blue or red regions of the spectrum in all complexes which may be considered as evidence for the complex formation. Also, new bands were observed in the spectra of the complexes which are listed in Table S3.

3.2.3.1. Mono- and homo-binuclear complexes. The effective magnetic moment values of the copper(II) complexes (**1** and **2**) are in the range of 1.82–1.97 BM [29, 43]. The electronic spectrum of **1** showed a band at 472 nm, which may be assigned to the ${}^2\text{B}_{1g} \rightarrow {}^2\text{B}_{2g}$ transition in a square planar geometry [57]. Complex **2** showed two absorption bands at 440 and 558 nm, which may be assigned to the ${}^2\text{B}_{1g} \rightarrow {}^2\text{E}_g$ and ${}^2\text{B}_{1g} \rightarrow {}^2\text{B}_{2g}$ transitions, respectively, corresponding to a distorted octahedral geometry [29, 58]. X-band ESR spectrum of $[(\text{HL})\text{Cu}(\text{NO}_3)(\text{H}_2\text{O})_2]\cdot\text{EtOH}$ (**2**) (Figure S3) was recorded in the solid state at 25 °C. The spectrum of the complex exhibits two signals at $g = 2.18$ and $g = 2.07$. The shape of the spectrum is consistent with octahedral geometry around Cu(II) in the complex [26, 29, 43]. The spin Hamiltonian parameters of the complex were calculated and are summarized in Table 1. The ESR spectrum of the complex exhibited axial g -tensor parameters with $g_{\parallel} > g_{\perp} > 2.0023$. The exchange

Table 1. ESR data of copper(II) and oxovanadium(IV) complexes at room temperature.

Complex	g_{\parallel}	g_{\perp}	$A_{\parallel} \times 10^{-4} \text{ (cm}^{-1}\text{)}$	$A_{\perp} \times 10^{-4} \text{ (cm}^{-1}\text{)}$	α^2	β^2
[(HL)Cu(NO ₃)(H ₂ O) ₂]-EtOH (2)	2.18	2.07	140	70	0.64	0.75
[(HL)VO(OH)(EtOH)] (8)	1.97	1.99	160	75	0.61	0.94

interaction parameter term G , estimated from the expression $G = (g_{\parallel} - 2.0023)/(g_{\perp} - 2.0023)$ [59] is 2.62, indicating a Cu...Cu exchange interaction [58].

Molecular orbital coefficients, α^2 (a measure of the covalency of the in-plane σ -bonding between copper 3d orbital and the ligand orbitals) and β^2 (covalent in-plane π -bonding), were calculated [60]. The lower value of α^2 compared to β^2 indicates that the in-plane σ -bonding is more covalent than the in-plane π -bonding. These data are in agreement with the data reported earlier [1, 29, 58].

The effective magnetic moment of the nickel(II) complex (**3**) is 3.4 BM which lies in the range (3.2–4.1 BM) reported for tetrahedral geometry [61]. The electronic spectrum of **3** showed one band at 784 nm which may be assigned to the ${}^3T_1(F) \rightarrow {}^3T_1(P)$ transition in a tetrahedral geometry [19, 39].

The effective magnetic moment values of the cobalt(II) complexes (**4** and **5**) are 3.5–3.6 BM, lower than expected for tetrahedral complexes (4.4–4.8 BM). The lower values of magnetic moments may point to a not purely tetrahedral geometry of Co(II) and a tendency towards square-planar geometry [62], which is characterized by lower magnetic moments (2.1–2.8 BM) [63]. The tetrahedral geometry is supported by the electronic spectra of the complexes that showed bands in the range of 530–575 nm, which may be assigned to the ${}^4A_2(F) \rightarrow {}^4T_1(P)$ electronic transition in a tetrahedral geometry [64].

The effective magnetic moment of the iron(III) complex (**6**) is 5.9 BM which is consistent with the presence of five unpaired electrons in the Fe(III) ion in an octahedral geometry [61]. The electronic spectrum of **6** showed one band at 492 nm, within the range reported for octahedral complexes [49]. It was not possible to identify the type of the d–d transition. This is due to a strong charge transfer (CT) band tailing from UV-region to the visible region [18, 26].

Zinc(II) complex **7** is diamagnetic as expected. The electronic spectrum of the complex showed one band at 440 nm, which may be attributed to CT transitions.

The effective magnetic moment value of the oxovanadium(IV) complex (**8**) is 1.4 BM. The value is lower than reported values (1.74–2.10 BM), indicating an interaction of the oxovanadium(IV) ion with neighboring ions [65]. The electronic spectrum of the complex (**8**) showed new bands at 449 and 525 nm that may be assigned to the ${}^2B_2 \rightarrow {}^2E$ and ${}^2B_{2g} \rightarrow {}^2B_1$ transitions, respectively, in an octahedral geometry [64]. In addition, the V=O stretching frequency for the complex at 952 cm^{-1} supports octahedral geometry of the complex [47, 66, 67]. The X-band ESR spectrum of a powdered sample of **8** at room temperature (Figure S3) showed a broad band without resolved hyperfine structure. In particular, the hyperfine coupling with the nearby ${}^{51}\text{V}$ ($I = 7/2$) nucleus is not observed. The absence of vanadium hyperfine coupling is common in solid state samples [68] and may be attributed to the simultaneous flipping of neighboring electron spins [69] or to strong exchange interactions, which average out the interaction with the nuclei. The g and A values (Table 1) in addition to the energy of d–d transition were used to evaluate the molecular orbital coefficients α^2 , β^2 for the complex [70]. The calculated values $\alpha^2 = 0.62$ and $\beta^2 = 0.90$ agree well with those reported for octahedral configuration around oxovanadium(IV) [65]. The lower value of α^2 compared to β^2 indicates that the in-plane σ -bonding is more covalent than the in-plane π -bonding [47].

The dioxouranium(VI) complexes (**9** and **10**) are diamagnetic as expected. The electronic spectra of the complexes showed new absorptions at 441–473 nm, which may be attributed to an electronic transition from the apical oxygens to f-orbitals of the uranium(VI) or due to a CT transition from the ligand to uranium(VI) [25, 26, 28].

3.2.3.2. Heterobinuclear complexes. Since the mononuclear dioxouranium(VI) complex [(HL)-(UO₂)(OAc)(H₂O)]·5H₂O (**9**) has free coordinating sites, it can be used as a chelating agent towards copper(II), nickel(II), cobalt(II), and iron(III) to yield heterobinuclear complexes. The complex ligand

(9) is diamagnetic, so any magnetic moments of the heteronuclear complexes can be attributed to introduction of metal cations.

The reactions of **9** with CuCl_2 , $\text{NiCl}_2 \cdot 6\text{H}_2\text{O}$, $\text{CoCl}_2 \cdot 6\text{H}_2\text{O}$, and $\text{FeCl}_3 \cdot 6\text{H}_2\text{O}$ in a 1 : 1 molar ratio in the presence of LiOH yielded the heterobinuclear complexes, $[(\text{L})(\text{UO}_2)\text{Cu}(\text{OAc})\text{Cl}(\text{H}_2\text{O})(\text{MeOH})] \cdot \text{MeOH}$ (**11**), $[(\text{L})(\text{UO}_2)\text{Ni}(\text{OAc})\text{Cl}(\text{H}_2\text{O})_4] \cdot 3\text{H}_2\text{O}$ (**12**), $[(\text{L})(\text{UO}_2)\text{Co}(\text{OAc})\text{Cl}(\text{H}_2\text{O})_2] \cdot 2.5\text{H}_2\text{O}$ (**13**) and $[(\text{L})(\text{UO}_2)\text{Fe}(\text{OAc})\text{Cl}_2(\text{H}_2\text{O})_2(\text{MeOH})_2]$ (**14**).

Electronic spectra of the heterobinuclear complexes showed two absorptions. The first is similar to that observed in **9**. The second is related to d–d transition of the introduced metal ions which was supported by magnetic moment measurements. The magnetic moment of **11** is 1.8 BM [29, 43]. The electronic spectrum of the complex showed a new band at 573 nm which may be assigned to the ${}^2\text{B}_{1g} \rightarrow {}^2\text{A}_{1g}$ transition in a square planar geometry [25, 58].

The magnetic moment of **12** is 2.8 BM which indicates the presence of two unpaired electrons per Ni(II), also confirming its octahedral geometry [1]. The electronic spectrum of the complex showed a band at 530 nm which may be assigned to the ${}^3\text{A}_{2g}(\text{F}) \rightarrow {}^3\text{T}_{1g}(\text{P})$ transition in an octahedral geometry [71].

The magnetic moment of **13** is 2.56 BM which indicates a square-planar geometry [49]. The electronic spectrum of the complex showed one band at 545 nm which may be assigned to the ${}^2\text{A}_{1g} \rightarrow {}^2\text{B}_{2g}$ transition in a square-planar geometry [49, 72].

The magnetic moment of **14** is 5.3 BM indicating octahedral arrangement with a slight antiferromagnetic interaction [27]. The electronic spectrum of the complex showed one band at 452 nm which indicates octahedral geometry [62].

3.2.4. Thermal analysis

Thermal gravimetric analysis indicates whether the water and solvent molecules are in the inner or outer coordination sphere of the central metal ion [1, 27]. Complexes **2**, **10**, **11**, **12**, and **13** were taken as representative examples for thermal analysis. Figure S4 shows the thermogram of **11**. The thermal analyses of the complexes (Table S5) are in agreement with the formulas as suggested from elemental analyses. The first stage of decomposition of the complexes extends up to 146 °C corresponding to loss of non-coordinated water or solvated ethanol or methanol. The second stage of decomposition extends up to 289 °C corresponding to loss of coordinated water and/or methanol molecules which is accompanied with the elimination of HCl (**12**). The third stage of decomposition extends up to 412 °C corresponding to loss of the coordinated anions as HCl, HNO_3 , or AcOH. The decomposition pattern of **2** is shown in Scheme 2.

3.2.5. Mass spectra

Complexes **1**, **3**, **6**, **9**, **10**, and **12** were chosen as representative complexes for mass spectral studies as they include all types of the synthesized complexes [mononuclear (**1**, **6**, and **9**), homo-binuclear complexes (**3** and **10**) and hetero-binuclear complex (**12**)]. The mass spectra of **1**, **6**, **9**, and **12** are depicted in Figure S2.

The mass spectrum of **1** showed the molecular ion peak at $m/e = 455$ (Calcd = 454.93) with 15.57% abundance. The peaks observed at $m/e = 456$ [M + 1] and 457 [M + 2] may be due to isotopic species. The fragments observed at $m/e = 409$ (15.57%), 392 (14.21%) and 363 (16.39) correspond to [M–EtOH], [M– HNO_3] and [M– $\text{C}_6\text{H}_4\text{NH}_2$], respectively. The peak at $m/e = 79$ (20.22%) represents CuO. Finally, the peak at $m/e = 65$ (31.69%) is due to Cu. Proposal degradation steps of **1** are shown in Scheme S2.

The mass spectrum of **3** showed the molecular ion peak at $m/e = 452$ (Calcd = 451.78) with 32.83% abundance which corresponds to [M– $2\text{H}_2\text{O}$]. The peak observed at $m/e = 453$ may be due to isotopic species. The fragments observed at $m/e = 437$ (38.38%) and 400 (402; 28.79%) correspond to [M– CH_3] and [M– H_2O – 2OH], respectively. The peak at $m/e = 76$ (28.79%) represents NiO. Finally, the peak at $m/e = 59$ (27.78%) is due to Ni.

The mass spectrum of **6** showed the molecular ion peak at $m/e = 428$ (Calcd = 428.08) with 37.25% abundance. The peaks observed at $m/e = 429$ [M + 1] and 430 [M + 2] may be due to isotopic species. The fragments observed at $m/e = 411$ (37.25%), 410 (58.17%), 393 (52.94%), 357 (356; 37.25%) and 336

(337; 47.71%) correspond to [M–OH], [M–H₂O], [M–Cl], [M–Cl₂] and [M–C₆H₄NH₂], respectively. The peak at $m/e = 72$ (47.71%) represents FeO. Finally, the peak at $m/e = 56$ (50.98%) is due to Fe.

The mass spectrum of **9** showed the molecular ion peak at $m/e = 631$ (Calcd = 630.48) with 23.8% abundance which corresponds to [M–5H₂O]. The peaks observed at $m/e = 632$ and 633 may be due to isotopic species. The fragments observed at $m/e = 616$ (16.57%), 588 (589; 18.98%), 553 (18.07%) and 539 (26.2%) correspond to [M–CH₃], [M–COCH₃], [M–H₂O–AcOH], and [M–C₆H₄NH₂], respectively. The peaks at $m/e = 270$ (21.99%) and 238 (25.9%) represent UO₂ and U, respectively.

Similarly, the mass spectra of **10** and **12** showed the molecular ion peaks at $m/e = 911$; 44.29% (Calcd = 910.5) and 779; 63.79% (Calcd = 778.65), which correspond to [M–5H₂O] and [M–3H₂O], respectively. The peaks observed at $m/e = 912$ and 913 (**10**) and at $m/e = 780$ and 781 (**12**) may be due to isotopic species. In **10**, the fragments observed at $m/e = 877$ (878; 73.57%), 857 (38.57%), 819 (4.29%), 270 (12.14%), and 239 (18.57%) correspond to [M–2OH], [M–3H₂O], [M–C₆H₄NH₂], UO₂, and U, respectively. In **12**, the fragments observed at $m/e = 764$ (50%), 749 (750; 62.93%), 744 (67.24%), 719 (718; 46.55%), 687 (56.03%), and 648 (44.83%) correspond to [M–CH₃], [M–2CH₃], [M–Cl], [M–AcOH], [M–C₆H₄NH₂], and [M–4H₂O–AcOH], respectively. Thus, we can conclude that mass spectral data reinforce the conclusions drawn from analytical and spectral data.

Based on the above interpretation of elemental and thermal analyses and spectral data (infrared, electronic, mass, and ESR) as well as magnetic susceptibility measurements at room temperature and conductivity measurements, it is possible to draw tentative structures of the metal complexes. Figures 1–3 represent the proposed structures of the metal complexes.

3.3. Antimicrobial activity

The antimicrobial activities of the ligand and its metal complexes were investigated against *S. aureus* (ATCC 25923) and *B. subtilis* (ATCC 6635) as Gram-positive bacteria, *E. coli* (ATCC 25922) and *S. typhimurium* (ATCC 14028) as Gram-negative bacteria, yeast: *C. albicans* (ATCC 10231), and fungus: *A. fumigatus*. The results are listed in Table S6. The data in Table S6 reveal that the ligand and its metal complexes are inactive against *S. aureus* and *E. coli*. Against *S. typhimurium*, the ligand showed low activity while its oxovanadium(IV) complex showed moderate activity. Against *B. subtilis*, the ligand showed low activity. This activity is enhanced upon complexation with copper(II), nickel(II), iron(III), zinc(II), and oxovanadium(IV) and the order of activity is Fe(III) > VO(IV) > Ni(II) > Cu(II); cationic complex **1** > Zn(II) > Cu(II); neutral complex **2**. Generally, it can be concluded that chelation tends to make the ligand a more powerful bacterial agent. A possible explanation for this increase in the activity upon chelation is that, in chelated complex, the positive charge of the metal is partially shared with donors present on the ligands [20]. Generally, chelated complexes deactivate various cellular enzymes, which play a vital role in various metabolic pathways of these micro-organisms. Other factors such as solubility, conductivity and dipole moment, affected by the presence of metal ions, may also be reasons for increasing the biological activity of the metal complexes as compared to the ligand from which they are derived [20].

Against *C. albicans*, the ligand and all metal complexes showed high activity and most of the complexes are more active than the ligand. The order of activity for mono- and homo-binuclear complexes is Cu(II) > UO(VI) > VO(IV) > Fe(III) > Ni(II) > Zn(II) > Co(II) while for heterobinuclear complexes Cu(II) ≈ Co(II) > Ni(II) > Fe(III).

Against *A. fumigatus*, the ligand and most of its metal complexes have high activity and most complexes are more active than the ligand. The increased activity against *C. albicans* and *A. fumigatus* may be due to the formation of hydrogen bonds between the azomethine nitrogen or carbonyl oxygen with active centers of the cell constituents, resulting in interference with the normal cell process [24].

The minimum inhibitory concentration (MIC) was determined for the synthesized compounds and the results are listed in Table 2. Against *B. subtilis*, the ligand and **12** showed lower activity (MIC = 62–75 μg mL⁻¹), while **1–3** and **6–8** showed an intermediate activity (MIC = 39–50 μg mL⁻¹). Against *S. typhimurium*, the ligand showed a low activity (MIC = 88 μg mL⁻¹) and **8** showed intermediate activity (MIC = 66 μg mL⁻¹). Against *C. albicans*, the ligand and most of its complexes showed promising

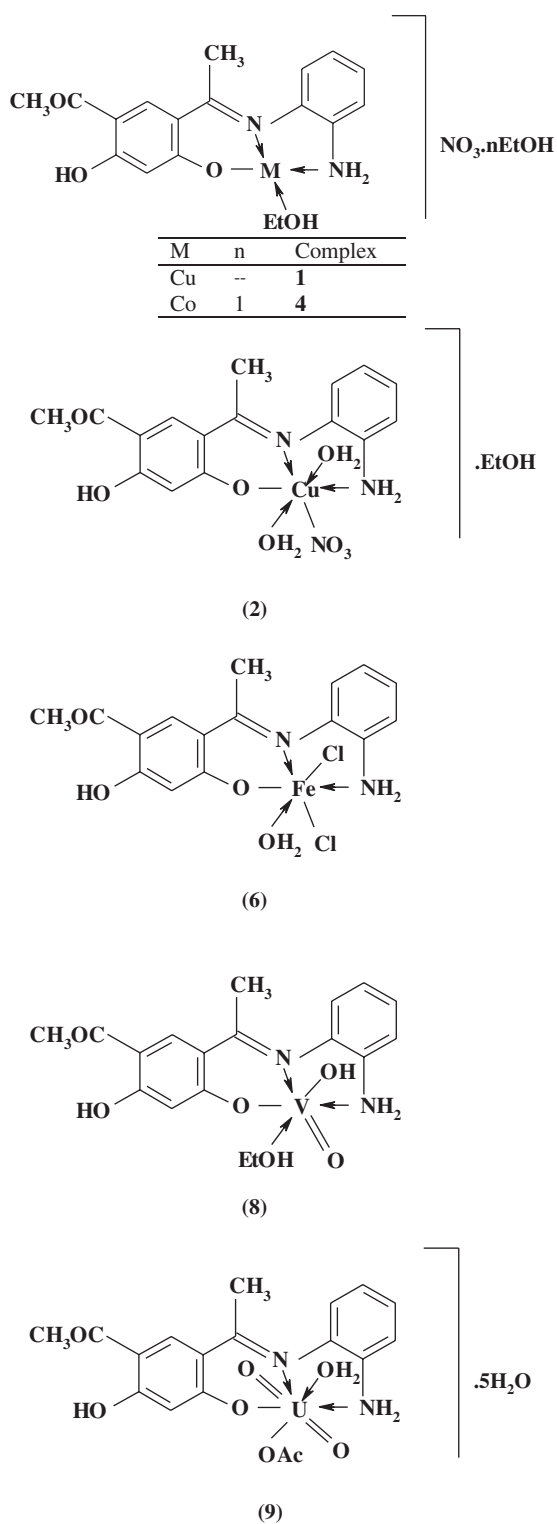


Figure 1. Proposed structures of the mononuclear complexes of H_2L .

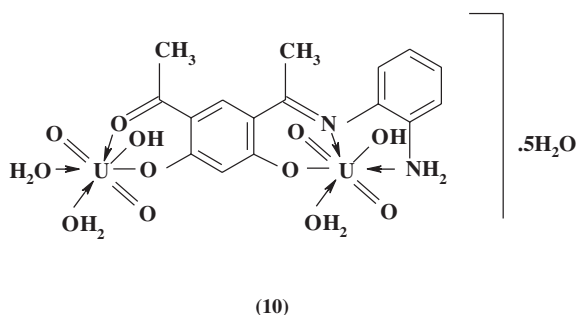
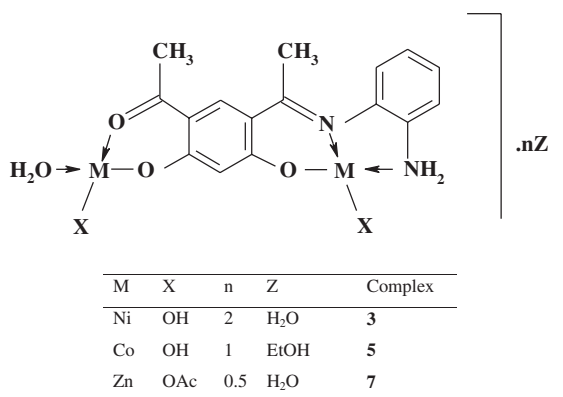


Figure 2. Proposed structures of the homo-binuclear complexes of H₂L.

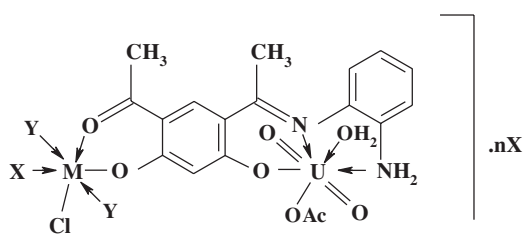
activity, especially **1** and **2** (MIC = 4–5 µg mL⁻¹). The other complexes showed intermediate to higher activity (MIC = 6–22 µg mL⁻¹). Finally, against *A. fumigatus*, the ligand showed an intermediate activity (MIC = 30 µg mL⁻¹) and the complexes showed moderate to high activity (MIC = 8–40 µg mL⁻¹).

1, **2**, and **12** seem to be promising as they showed antimicrobial activity and MIC values that are comparable to that of cycloheximide and, thus, can be further explored as specific antimicrobial drugs.

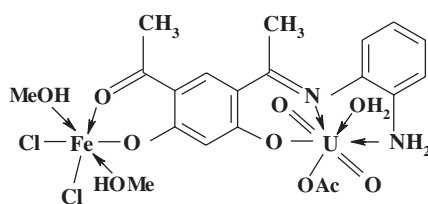
The obtained results are consistent with the previously reported metal complexes of similar Schiff bases which were tested *in vitro* for their antibacterial activities against bacteria or fungi (using disk diffusion method [20, 59, 73] or MIC method [21, 24, 74, 75]).

3.4. Antioxidant activity

DPPH is a stable free radical used for studying radical scavenging activity in chemical analysis [76], which is measured as IC₅₀ values. The antioxidant activity of the Schiff base and its complexes against DPPH radical was carried out with the hope to develop potential antioxidants and therapeutic agents. The DPPH radical shows a strong absorption at 517 nm in the visible spectrum due to the presence of an odd electron. As this electron becomes paired-off in the presence of a free radical scavenger, this absorption vanishes with respect to the number of electrons taken up. The DPPH scavenging ability of the synthesized compounds was compared with that of the well-known natural antioxidant ascorbic acid under the same experimental conditions. The results of the *in vitro* radical scavenging assay (Table 3) strongly support that the synthesized compounds exhibit antioxidant activity against DPPH radical. H₂L showed promising antioxidant activity (IC₅₀ = 118.1 µM) which is the highest among the complexes and higher than that of ascorbic acid. The IC₅₀ values for mononuclear and binuclear complexes are 151.3–175.4 and 208.2–240 µM, respectively. The order of antioxidant activity was H₂L > mononuclear



M	X	Y	n	Complex
Cu	MeOH	--	1	11
Ni	H ₂ O	H ₂ O	3	12
Co	H ₂ O	--	2.5	13



(14)

Figure 3. Proposed structures of the hetero-binuclear complexes of H₂L.

Table 2. Minimum inhibitory concentration (MIC) ($\mu\text{g mL}^{-1}$) of H₂L and its complexes.

Compound	Gram-(+) bacteria	Gram-(−) bacteria	Yeasts and fungi	
	<i>B. subtilis</i>	<i>S. typhimurium</i>	<i>C. albicans</i>	<i>A. fumigatus</i>
H ₂ L	75	88	10	30
[(HL)Cu(EtOH)]NO ₃ (1)	44	ND ^b	4	36
[(HL)Cu(NO ₃)(H ₂ O) ₂]-EtOH (2)	50	ND	5	ND
[(L)Ni ₃ (OH) ₂ (H ₂ O) ₃]-2H ₂ O (3)	42	ND	13	36
[(HL)Co(EtOH)]NO ₃ ·EtOH (4)	ND	ND	22	ND
[(L)Co ₂ (OH) ₂ (H ₂ O) ₃]-EtOH (5)	ND	ND	21	ND
[(HL)FeCl ₂ (H ₂ O)] (6)	39	ND	10	20
[(L)Zn ₃ (OAc) ₂ (H ₂ O)]·0.5H ₂ O (7)	47	ND	16	20
[(HL)V(OH)(EtOH)] (8)	40	66	7	40
[(HL)(UO ₂)(OAc)(H ₂ O)]·5H ₂ O (9)	ND	ND	6	25
[(L)(UO ₂) ₂ (OH) ₂ (H ₂ O) ₃]-5H ₂ O (10)	ND	ND	7	24
[(L)(UO ₂)Cu(OAc)Cl(H ₂ O)(MeOH)]·MeOH (11)	ND	ND	9	20
[(L)(UO ₂)Ni(OAc)Cl(H ₂ O) ₄]-3H ₂ O (12)	62	ND	11	8
[(L)(UO ₂)Co(OAc)Cl(H ₂ O) ₂]-2.5H ₂ O (13)	ND	ND	9	21
[(L)(UO ₂)Fe(OAc)Cl ₂ (H ₂ O)(MeOH) ₂] (14)	ND	ND	14	20
Control ^a	1	13	3	2

^aChloramphenicol in the case of Gram-positive bacteria, cephalothin in the case of Gram-negative bacteria and cycloheximide in the case of yeasts and fungi.

^bND = Not determined.

complexes > binuclear complexes. This order may be due to the presence of two phenolic OH groups in the ligand which donate a proton to DPPH and converts into the stable free radical [24]. Upon complexation, deprotonation occurs (for one OH group in mononuclear and two OH groups in binuclear complexes), lowering the antioxidant activity. The obtained results are consistent with those obtained by Raj *et al.* [24] in a previous study including Cu(II), Co(II), Ni(II), and Zn(II) complexes of bicompartamental

Table 3. Antioxidant activity of H₂L and its complexes.

Compound	DPPH assay IC ₅₀ (μM) ^a	
	30 min	60 min
H ₂ L	118.1 ± 3.51	105.3 ± 6.41
[(HL)Cu(EtOH)]NO ₃ (1)	151.3 ± 2.5	133.4 ± 1.4
[(HL)Cu(NO ₃)(H ₂ O) ₂]-EtOH (2)	160.5 ± 3.1	142 ± 4.2
[(L)Ni ₂ (OH) ₂ (H ₂ O) ₂]-2H ₂ O (3)	240 ± 0.4	216 ± 1.2
[(HL)Co(EtOH)]NO ₃ -EtOH (4)	162.5 ± 0.25	145.3 ± 0.07
[(L)Co ₂ (OH) ₂ (H ₂ O) ₂]-EtOH (5)	220.1 ± 1.3	200 ± 1.4
[(HL)FeCl ₂ (H ₂ O)] (6)	170 ± 1.3	158.3 ± 2.4
[(HL)VO(OH)(EtOH)] (8)	175.4 ± 4.2	162.6 ± 4.1
[(L)(UO ₂)Cu(OAc)Cl(H ₂ O)(MeOH)]-MeOH (11)	230.2 ± 2.1	205.4 ± 4.3
[(L)(UO ₂)Ni(OAc)Cl(H ₂ O) ₄]-3H ₂ O (12)	216.2 ± 1.2	198.4 ± 3.05
[(L)(UO ₂)Co(OAc)Cl(H ₂ O) ₃]-2.5H ₂ O (13)	208.2 ± 1.5	190.1 ± 3.5
[(L)(UO ₂)Fe(OAc)Cl ₂ (H ₂ O)(MeOH) ₂] (14)	235 ± 0.05	204.1 ± 4.2
Ascorbic acid	126.4 ± 11.3	122.5 ± 10.4

^aIC₅₀ values were determined by linear regression analysis.

Table 4. In vitro cytotoxicity of H₂L and its complexes on Ehrlich Ascites Carcinoma cell line.

Compound	IC ₅₀ (mg mL ⁻¹)
H ₂ L	85.36
[(HL)Cu(EtOH)]NO ₃ (1)	21.34
[(HL)Cu(NO ₃)(H ₂ O) ₂]-EtOH (2)	25.05
[(L)Ni ₂ (OH) ₂ (H ₂ O) ₂]-2H ₂ O (3)	18.48
[(HL)Co(EtOH)]NO ₃ -EtOH (4)	20.33
[(L)Co ₂ (OH) ₂ (H ₂ O) ₂]-EtOH (5)	15.73
[(HL)FeCl ₂ (H ₂ O)] (6)	27.46
[(L)Zn ₂ (OAc) ₂ (H ₂ O)]-0.5H ₂ O (7)	22.06
[(HL)VO(OH)(EtOH)] (8)	16.22
[(HL)(UO ₂)(OAc)(H ₂ O)]-5H ₂ O (9)	15.38
[(L)(UO ₂) ₂ (OH) ₂ (H ₂ O) ₃]-5H ₂ O (10)	17.4
[(L)(UO ₂)Cu(OAc)Cl(H ₂ O)(MeOH)]-MeOH (11)	19.65
[(L)(UO ₂)Ni(OAc)Cl(H ₂ O) ₄]-3H ₂ O (12)	22.01
[(L)(UO ₂)Co(OAc)Cl(H ₂ O) ₃]-2.5H ₂ O (13)	24.39
[(L)(UO ₂)Fe(OAc)Cl ₂ (H ₂ O)(MeOH) ₂] (14)	27.33
Cisplatin	5

Note: IC₅₀ = inhibition concentration 50%.

Schiff bases derived from 4,6-diacetylresorcinol. Finally, the difference in the activity of the metal complexes may be due to the coordination environment and the redox properties. In general, the redox properties of the complex depend on chelate ring size, axial ligation, and degree of unsaturation in the chelate ring [77].

3.5. Antitumor activity

The antitumor activities of the Schiff base and its complexes were tested on Ehrlich Ascites Carcinoma and the results are listed in Table 4. The ligand showed moderate activity (IC₅₀ = 85.36 mg mL⁻¹), while complexes showed higher activity (IC₅₀ = 15.38–27.46 mg mL⁻¹).

The activity of the complexes is due to the metal ions which enhance the anticancer behavior as it is evidenced by the lower IC₅₀ values of the complexes compared with free H₂L. The higher activity of the complexes than H₂L may be attributed to the extended planar structure induced by the π-π* conjugation resulting from chelation of the metal ion with the ligand [78, 79]. In addition, enhanced activity of metal complexes may also be due to higher lipophilic nature of the complexes, increased due to chelation with faster diffusion of the chelates through the cell membrane [80]. Complexes **5**, **8**, and **9** are promising as they showed low toxicity in relation to *cis*-platin.

4. Conclusion

The condensation of 4,6-diacetylresorcinol with *o*-phenylenediamine in molar ratio 1:1 afforded the new Schiff base H₂L. The reactions of the Schiff base with copper(II), nickel(II), cobalt(II), iron(III), zinc(II), oxovanadium(IV), and dioxouranium(VI) in the absence and presence of LiOH yielded mono- and bi-nuclear complexes with different coordination sites. The mononuclear dioxouranium(VI) complex [(HL)-(UO₂)(OAc)(H₂O)]·5H₂O was used to synthesize heterobinuclear complexes. The ligand and its metal complexes were characterized by elemental analyses, IR, ¹H-, and ¹³C-NMR, electronic, ESR, and mass spectra, conductivity and magnetic susceptibility measurements as well as thermal analysis. The ligand and its metal complexes showed promising antimicrobial and antioxidant activities. The ligand and metal complexes showed antitumor activity against Ehrlich Acites Carcinoma.

Disclosure statement

No potential conflict of interest was reported by the author.

References

- [1] M. Shebl. *Spectrochim. Acta, Part A*, **117**, 127 (2014).
- [2] C. Liang, J. Xia, D. Lei, X. Li, Q. Yao, J. Gao. *Eur. J. Med. Chem.*, **74**, 742 (2014).
- [3] M.A.S. Omer, J. Liu, W. Deng, N. Jin. *Polyhedron*, **69**, 10 (2014).
- [4] P. Fantucci, V. Valenti. *J. Am. Chem. Soc.*, **98**, 3832 (1976).
- [5] D. Chen, A.E. Martell, Y. Sun. *Inorg. Chem.*, **28**, 2647 (1989).
- [6] E. Kimura, S. Wada, M. Shionoya, Y. Okazaki. *Inorg. Chem.*, **33**, 770 (1994).
- [7] S.L. Lambert, C. Spiro, R.R. Gagne, D.N. Hendrickson. *Inorg. Chem.*, **21**, 68 (1982).
- [8] Z. Abbasi, M. Behzad, A. Ghaffari, H.A. Rudbari, G. Bruno. *Inorg. Chim. Acta*, **414**, 78 (2014).
- [9] G. Grivani, S. Delkosh, K. Fejfarová, M. Dušek, A.D. Khalaji. *Inorg. Chem. Commun.*, **27**, 82 (2013).
- [10] N. Zhang, Y. Fan, Z. Zhang, J. Zuo, P. Zhang, Q. Wang, S. Liu, C. Bi. *Inorg. Chem. Commun.*, **22**, 68 (2012).
- [11] O. Kahn. *Adv. Inorg. Chem.*, **43**, 179 (1995).
- [12] K.S. Murray. *Adv. Inorg. Chem.*, **43**, 261 (1995).
- [13] H. Ökawa, H. Furutachi, D.E. Fenton. *Coord. Chem. Rev.*, **174**, 51 (1998).
- [14] W.R. Browne, R. Hage, J.G. Vos. *Coord. Chem. Rev.*, **250**, 1653 (2006).
- [15] V. Rajendiran, R. Karthik, M. Palaniandavar, H. Stoeckli-Evans, V. Subbarayan Periasamy, M.A. Akbarsha, B.S. Srinag, H. Krishnamurthy. *Inorg. Chem.*, **46**, 8208 (2007).
- [16] M. Trivedi, D.S. Pandey, N.P. Rath. *Inorg. Chim. Acta*, **362**, 284 (2009).
- [17] T. Ruffer, B. Bräuer, F.E. Eya'ane Meva, L. Sorace. *Inorg. Chim. Acta*, **362**, 563 (2009).
- [18] A.A.A. Emara, O.M.I. Adly. *Transition Met. Chem.*, **32**, 889 (2007).
- [19] A.A.A. Emara, A.A.A. Abou-Hussen. *Spectrochim. Acta, Part A*, **64**, 1010 (2006).
- [20] A.A.A. Emara. *Spectrochim. Acta, Part A*, **77**, 117 (2010).
- [21] J.H. Pandya, R.N. Jadeja, K.J. Ganatra. *J. Saudi Chem. Soc.*, **18**, 190 (2014).
- [22] N.V. Kulkarni, M.P. Sathisha, S. Budagumpi, G.S. Kurdekar, V.K. Revankar. *J. Coord. Chem.*, **63**, 1451 (2010).
- [23] P.V. Rao, S. Ammanni, S. Kalidasu. *E-J. Chem.*, **8**, 470 (2011).
- [24] K.M. Raj, B. Vivekanand, G.Y. Nagesh, B.H.M. Mruthyunjayswamy. *J. Mol. Struct.*, **1059**, 280 (2014).
- [25] M. Shebl. *Spectrochim. Acta, Part A*, **70**, 850 (2008).
- [26] M. Shebl. *Spectrochim. Acta, Part A*, **73**, 313 (2009).
- [27] M. Shebl. *J. Coord. Chem.*, **62**, 3217 (2009).
- [28] M. Shebl, H.S. Seleem, B.A. El-Shetary. *Spectrochim. Acta, Part A*, **75**, 428 (2010).
- [29] M. Shebl, M.A. El-ghamry, S.M.E. Khalil, M.A.A. Kishk. *Spectrochim. Acta, Part A*, **126**, 232 (2014).
- [30] F.E. Mabbs, D.I. Machin. *Magnetism and Transition Metal Complexes*, pp. 5–6, Chapman and Hall, London (1973).
- [31] A.U. Atta-ur-Rahman, M.I. Choudhary, W.J. Thomson. *Bioassay Techniques For Drug Development*, p. 14, Harwood Academic Publishers, The Netherlands (2001).
- [32] K.M. Khan, Z.S. Saify, A.K. Zeesha, M. Ahmed, M. Saeed, M. Schick, H.J. Kohlbau, W. Voelter. *Arzneim. Forsch.*, **50**, 915 (2000).
- [33] J.M. Andrews. *J. Antimicrob. Chemother.*, **48**, 5 (2001).
- [34] T. Takao, F. Kitatani, N. Watanabe, A. Yagi, K. Sakata. *Biosci., Biotechnol. Biochem.*, **58**, 1780 (1994).
- [35] W.F.V. Mclimans, F.L. Glover, G.W. Rake. *J. Immunol.*, **79**, 428 (1957).
- [36] J.R. Platt. *J. Chem. Phys.*, **17**, 484 (1949).

- [37] E. Pretsch, T. Clerc. *Tables of Spectral Data for Structure Determination of Organic Compounds*, Springer-Verlag, Berlin (1983).
- [38] A.A.A. Abu-Hussen, A.A.A. Emara. *J. Coord. Chem.*, **57**, 973 (2004).
- [39] A.A.A. Emara, B.A. El-Sayed, E.A.E. Ahmed. *Spectrochim. Acta, Part A*, **69**, 757 (2008).
- [40] J. Anaconda, J. Santaella. *Spectrochim. Acta, Part A*, **115**, 800 (2013).
- [41] M. Shebl, S.M.E. Khalil, A. Taha, M.A.N. Mahdi. *J. Mol. Struct.*, **1027**, 140 (2012).
- [42] M. Shebl, S.M.E. Khalil, A. Taha, M.A.N. Mahdi. *J. Am. Sci.*, **8**, 183 (2012).
- [43] M. Shebl, S.M.E. Khalil, A. Taha, M.A.N. Mahdi. *Spectrochim. Acta, Part A*, **113**, 356 (2013).
- [44] K. Nakamoto. *Infrared and Raman Spectra of Inorganic and Coordination Compounds*, 5th Edn, p. 256, John Wiley and Sons, New York (1997).
- [45] T. Rosu, E. Pahontu, D. Ilies, R. Georgescu, M. Mocanu, M. Leabu, S. Shova, A. Gulea. *Eur. J. Med. Chem.*, **53**, 380 (2012).
- [46] H.S. Seleem, B.A. El-Shetary, M. Shebl. *Heteroatom Chem.*, **18**, 100 (2007).
- [47] M. Shebl, S.M.E. Khalil. *Monatsh. Chem.*, **146**, 15 (2015).
- [48] S.M.E. Khalil, M. Shebl, F.S. Al-Gohani. *Acta Chim. Slov.*, **57**, 716 (2010).
- [49] M. Shebl, S.M.E. Khalil, S.A. Ahmed, H.A.A. Medien. *J. Mol. Struct.*, **980**, 39 (2010).
- [50] M. Shebl, S.M.E. Khalil, F.S. Al-Gohani. *J. Mol. Struct.*, **980**, 78 (2010).
- [51] S.P. McGlynn, J.K. Smith, W.C. Neely. *J. Chem. Phys.*, **35**, 105 (1961).
- [52] L.H. Jones. *Spectrochim. Acta, Part A*, **10**, 395 (1958).
- [53] M.M. Mashaly, Z.H. Abd El-Wahab, A.A. Faheim. *J. Chin. Chem. Soc.*, **51**, 1 (2004).
- [54] W.J. Geary. *Coord. Chem. Rev.*, **7**, 81 (1971).
- [55] (a) N.M. El-Metwally, A.A. El-Asmy. *J. Coord. Chem.*, **59**, 1591 (2006); (b) M.M. Hassanien, I.M. Gabr, M.H. Abdel-Rhman, A.A. El-Asmy. *Spectrochim. Acta, Part A*, **71**, 73 (2008).
- [56] (a) G.A.A. Al-Hazmi, M.S. El-Shahawi, I.M. Gabr, A.A. El-Asmy. *J. Coord. Chem.*, **58**, 713 (2005); (b) A.A. El-Asmy, N.M. El-Metwally, G.A. Al-Hazmi. *Transition Met. Chem.*, **31**, 673 (2006).
- [57] A.A. El-Asmy, M.A. Abdallah, Sh.A. Mandour, K.M. Ibrahim. *Synth. React. Inorg. Met.-Org. Nano-Met. Chem.*, **40**, 675 (2010).
- [58] M. Shebl, M.A. Ibrahim, S.M.E. Khalil, S.L. Stefan, H. Habib. *Spectrochim. Acta, Part A*, **115**, 399 (2013).
- [59] V.B. Badwaik, R.D. Deshmukh, A.S. Aswar. *J. Coord. Chem.*, **62**, 2037 (2009).
- [60] C.J. Carrano, C.M. Nunn, R. Quan, J.A. Bonadies, V.L. Pecoraro. *Inorg. Chem.*, **29**, 944 (1990).
- [61] F.A. Cotton, G. Wilkinson. *Advanced Inorganic Chemistry. A Comprehensive Text*, 4th Edn, p. 789, 761, John Wiley and Sons, New York (1986).
- [62] S.M.E. Khalil, H.S. Seleem, B.A. El-Shetary, M. Shebl. *J. Coord. Chem.*, **55**, 883 (2002).
- [63] J.C. Bailar, H.J. Emeleus, R. Nyholm, A.F. Trotman-Dickenson. *Comprehensive Inorganic Chemistry*, Vol. 3, 1st Edn, p. 1093, Pergamon Press, New York (1975).
- [64] O.A. El-Gammal, R.M. El-Shazly, F.E. El-Morsy, A.A. El-Asmy. *J. Mol. Struct.*, **998**, 20 (2011).
- [65] N.M. El-Metwally, R.M. El-Shazly, I.M. Gabr, A.A. El-Asmy. *Spectrochim. Acta, Part A*, **61**, 1113 (2005).
- [66] C.J. Sarrano, J.A. Bonadies. *J. Am. Chem. Soc.*, **108**, 4088 (1986).
- [67] S. Ooi, M. Nishizawa, K. Matsumoto, H. Kuroya, K. Saito. *Bull. Chem. Soc. Jpn.*, **52**, 452 (1979).
- [68] Y. Zhanglin, M. Forissier, J.C. Vedrine, J.C. Volta. *J. Catal.*, **145**, 267 (1994).
- [69] A. Bencini, D. Gatteschi. *EPR of Exchange Coupled Systems*, Springer-Verlag, Berlin (1990).
- [70] T.F. Yen. *Electron Spin Resonance of Metal Complexes*, 1st Edn, p. 111, Plenum Press, New York (1969).
- [71] P.P. Netalkar, A. Kamath, S.P. Netalkar, V.K. Revankar. *Spectrochim. Acta, Part A*, **97**, 762 (2012).
- [72] A.A. Abou-Hussen, N.M. El-Metwally, E.M. Saad, A.A. El-Asmy. *J. Coord. Chem.*, **58**, 1735 (2005).
- [73] Y.-L. Sang, X.-S. Lin. *J. Coord. Chem.*, **63**, 315 (2010).
- [74] A.D. Kulkarni, G.B. Bagihalli, S.A. Patil, P.S. Badami. *J. Coord. Chem.*, **62**, 3060 (2009).
- [75] A.D. Kulkarni, P.G. Avaji, G.B. Bagihalli, S.A. Patil, P.S. Badami. *J. Coord. Chem.*, **62**, 481 (2009).
- [76] S.B. Bukhari, S. Memon, M. Mahroof-Tahir, M.I. Bhangar. *Spectrochim. Acta, Part A*, **71**, 1901 (2009).
- [77] R.P. John, A. Sreekanth, V. Rajakannan, T.A. Ajith, M.R.P. Kurup. *Polyhedron*, **23**, 2549 (2004).
- [78] E. Ramachandran, D.S. Raja, N.S.P. Bhuvanesh, K. Natarajan. *Eur. J. Med. Chem.*, **64**, 179 (2013).
- [79] S. Sathiyaraj, K. Sampath, R.J. Butcher, R. Pallepogu, C. Jayabalakrishnan. *Eur. J. Med. Chem.*, **64**, 81 (2013).
- [80] N.E.A. El-Gamel. *RSC Adv.*, **2**, 5870 (2012).